A sheet erodibility parameter for water erosion modeling in regions with low intensity rain

Mohammad H. Hussein

ABSTRACT

Soil erodibility reflects the soil effect on the detachment process by rainfall and runoff; an evaluation of this parameter for single storm events was carried out using natural runoff plot data collected for two rainfall seasons in northern Iraq. The region is characterized by a semiarid Mediterranean-type climate with normal rainfall intensity below 20 mm/h and dominant sheet erosion on agricultural land. The plots were three 30×3 m and three 10×3 m, in fallow, situated on a 6% uniform slope; the soil at the site has a silty clay loam texture and belongs to the Calciorthid suborder. Sheet erosion rate was assumed linearly proportional to the storm power and the sheet flow power; a steady-state turbulent and kinematic sheet flow was also assumed. The results indicated a dominant detachment by rainfall with a substantial variability in storm by storm calculated sheet erodibility. The two-parameter lognormal probability distribution fitted the obtained sheet erodibility values reasonably well. Using this probability distribution, a representative sheet erodibility value of 0.056×10^{-3} kg/J was obtained for use at the experimental site.

Key words | Mediterranean climate, runoff plots, sheet/interrill erodibility, sheet flow, water erosion models

Mohammad H. Hussein
Department of Soil and Water,
College of Agriculture,
Babylon University,
Hilla-Iraq
E-mail: *husseinmohammad@yahoo.com*

INTRODUCTION

Soil properties influence the detachment, transport and deposition processes in water erosion. In water erosion models, the term soil erodibility is mainly used to reflect the soil effect on the detachment process by water erosion (Foster 1982). Soil properties known to affect its erodibility include primary particle size distribution, soil organic matter content, soil structure, soil biogeochemical properties such as soil mineralogy and pH, initial moisture content, and soil aging (Partheniades 1972; Alberts *et al.* 1995; Toorman 2001). Climate-related phenomena such as the freeze and thaw cycles also affect soil erodibility (Utley & Wynn 2008). Values for this parameter were obtained using natural runoff plots, rainfall simulation, and prediction models. In physically based water erosion models such as ANSWERS (Beasley *et al.* 1980), the erosion component of the CREAMS model (Foster *et al.* 1981), WEPP (Nearing *et al.* 1989), and EUROSEM (Morgan *et al.* 1998), sediment yield is predicted on a single storm basis. In such models, the selection of a proper soil erodibility parameter is imperative to prediction accuracy.

Low intensity rain is common in the Mediterranean-type climate which covers considerable areas in the six continents (Pettersen 1958). In these areas, sheet erosion is usually dominant on gently sloping land used mainly for agricultural purposes. Sheet erosion causes the removal of soil in thin layers and is caused by both raindrop splash and sheet flow (Wei *et al.* 2009). For the purpose of water erosion prediction in regions of low intensity rain, it is more important to predict the individual storms accurately because it is a relatively small number of intense storms which cause most of the erosion (Edwards 1985; Hussein 1996).

Although the subject of sheet/interrill erodibility has been widely researched (Laflen *et al.* 1991; Kinnell 1993; Alberts *et al.* 1995; Truman & Bradford 1995; Romero *et al.* 2007; Gumiere *et al.* 2009; Reichert *et al.* 2009), most of

doi: 10.2166/nh.2013.029

these studies used rainfall simulation on small laboratory plots. Few studies on this parameter under natural conditions have been carried out, especially in regions of low intensity rain. Such studies are essential since sheet erosion is normally the dominant form of water erosion on agricultural land in those regions.

Soil erosion by water is a major problem in northern Iraq (Hussein 1998; Jarjees *et al*. 2006). The purpose of this study was to evaluate soil erodibility under the condition of dominant sheet erosion in the low rainfall zone of north-western Iraq using natural runoff plot data; some guidelines for this parameter prediction under such a condition were proposed.

STUDY AREA AND DATA

Sediment yield data sets used in the sheet erodibility evaluation were collected from natural runoff plots in northern Iraq. The region has a semiarid Mediterranean-type climate. Rainfall season in the region usually extends from October to May. Normal rainfall intensity in the region is below 20 mm/h. The plot site is located at Hammam Al-Alil (36°9′59″ N, 43°15′25″ E) in the low rainfall zone of north-western Iraq (Figure 1(a)). Site elevation is about 250 m above mean sea level. Mean seasonal rainfall at the site is about 340 mm.

The experimental site was used primarily as grazing land, and the soil at the site is classified as fine, mixed, thermic, calcareous, Xerrollic Calciorthid. General soil characteristics are given in Table 1. Mica and chlorite are the dominant clay minerals followed by kaolinite and montmorillonite. Differences in mean temperature between winter and summer months are usually more than 20 °C. During the winter months, the minimum daily temperature occasionally drops below freezing point. During the summer months, the maximum daily temperature is usually above 40 °C.

At the site, six natural runoff plots in fallow were established on a 6% uniform slope area during the 1987–1988 rainfall season. The plots were three 30 × 3 m plots followed

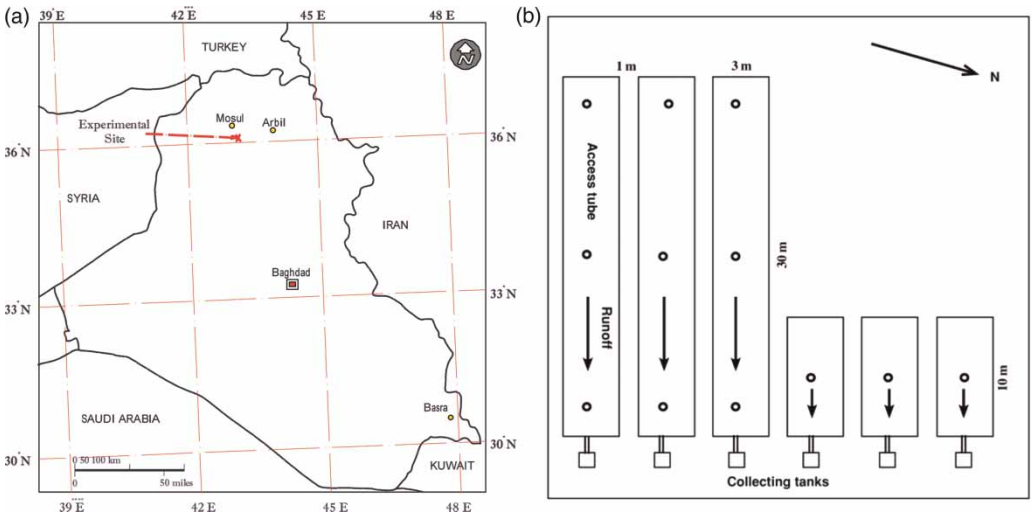

Figure 1 | (a) Map of Iraq showing the location of the experimental site. (b) Sketch of the field plot arrangement.

Table 1 | Soil characteristics at the experimental site (depth 0–0.3 m)

Soil particle size distribution											Soil moisture (V/V) at		
%clay	%silt	%vf sand	%sand	% Organic matter	% $CaCO_3$	% Gravel in surface soil	Bulk dens. (Mg/m^3)	MWD of agg. (mm)	CEC (Cmol/kg)	Sat. cond. (mm/h)	0.033 Mpa	1.5 Mpa	pH
36	44	2.4	17.6	1.5	28	13	1.3	0.26	24	37	0.3	0.09	7.6

MWD: mean weighted diameter; CEC: cation exchange capacity.

by three 10×3 m plots. The distance between adjacent plots was 1 m. The 30-m long plots were used to generate sufficient runoff during the storm event so that both sheet and rill erosion processes might occur on the plots. Each fall, and after rain showers had moistened the soil, the plots were tilled by spading, then smoothed and left in a fallow condition throughout the rainfall season. Herbicides were used to control weeds.

A nonrecording rain gauge was available at the site from the beginning of the experiment. An additional daily-type recording rain gauge has been available since the 1989–1990 rainfall season. Since no significant rilling on the plots was observed during the period of measurements, sheet erosion is assumed to be dominant on the plots.

After each runoff producing rainstorm, runoff volume in the collecting tank at each plot outlet was measured. Runoff was then mixed thoroughly and water samples were taken for analysis. Once in the laboratory, samples were dried and weighed to determine sediment mass.

Periodic soil moisture measurements with a neutron probe, at a 0.1-m depth interval, were carried out throughout the experiment. For this purpose, access tubes for soil moisture measurement were installed on all plots. Each of the large plots has three access tubes located at the upper, middle, and lower parts of the plot. The small plots have one access tube each situated at the middle part of the plot (Figure 1(b)).

METHODS

Sheet (interrill) erosion is caused by raindrop impact and shallow (sheet) overland flow. Detachment by raindrops and sheet flow is assumed linearly proportional to the effective sheet flow power (Yang 1972, 1973; Moore & Burch 1986; Hussein 1996; Zhang *et al.* 1998, 2003). From the principles of energy conservation, the effective sheet flow power is the sum of excess sheet flow power and storm power. Assuming 100% efficiency in total power availability for detachment, detachment of soil particles in the sheet erosion process may be expressed as:

$$D_s = K_s\{[(iEI_c)/3600] + [\tau V - (\tau V)_c]\} \quad (1)$$

where D_s = detachment rate by sheet erosion expressed in kg/m^2/s, K_s = sheet erodibility parameter (kg/J), i = fraction of soil surface exposed to direct raindrop impact, EI_c = storm power (J/m^2/h), E = storm kinetic energy per unit rainfall depth (J/m^2/mm rain), I_c = characteristic rainfall intensity for the storm (mm/h), τV = sheet flow power (J/m^2/s), τ = sheet flow shear stress (N/m^2), V = mean sheet flow velocity (m/s), and $(\tau V)_c$ = critical sheet flow power below which no detachment by sheet flow occurs (J/m^2/s).

A rainfall intensity for a duration equal to or greater than the time of concentration for the plots is a suitable characteristic rainfall intensity (Brodie & Egodawatta 2011). Hussein *et al.* (1994) found that a maximum 5-minute rainfall intensity (I_5) is a suitable characteristic rainfall intensity at this site.

Equation (1) is based on the assumption that as slope length increases, both storm power (EI_c) and sheet flow power (τV) become important in determining soil detachment rate in the sheet erosion process (Liu *et al.* 2005). K_s in Equation (1), as indicated by its unit, represents the mass of soil detached by sheet erosion in kg per one joule of work exerted by raindrop impact (and sheet flow where applicable). K_s is essentially a soil parameter which can be determined by measuring soil loss from sheet erosion under a detachment limiting condition. This condition means that sediment delivery by sheet erosion is limited by the sheet flow sediment load.

A steady-state condition is assumed due to the long storm duration normally associated with the low intensity rainfall. The sheet flow is assumed turbulent (Hussein *et al.* 1994) and kinematic. The kinematic assumption means that the friction slope is set equal to the land slope. The kinematic flow assumption is considered satisfactory for overland flow computations over small areas (Foster *et al.* 1968; Rovey & Woolhiser 1977). Hence:

$$\tau = \gamma y s \quad (2)$$

and

$$V = (\sigma x/y)/(3.6 \times 10^6) \quad (3)$$

where γ = weight density of water (N/m^3), y = sheet flow depth (m), s = sine of slope angle, σ = excess rainfall rate (mm/h) = rainfall rate – infiltration rate, and x = distance from the

upper end of slope (m). From Equations (2) and (3), the sheet flow power at a point x on the slope can be expressed as:

$$\tau V = \gamma \sigma x s/(3.6\times 10^6) \quad (4)$$

Accordingly, detachment rate at a point x on the slope (Equation (1)) may be rewritten as follows:

$$D_s = K_s(iEI_c)/(3.6\times 10^3) \qquad x \le x_c$$
$$D_s = K_s\{[(iEI_c)/(3.6\times 10^3)] + [\gamma \sigma s(x-x_c)/(3.6\times 10^6)]\} \qquad x > x_c \quad (5)$$

where x_c = distance from the upper end of slope before which no significant detachment by sheet flow occurs (m); K_s is calculated from Equations (6) and (7) as follows:

$$K_s = [D_s/(iEI_c)](3.6\times 10^3) \qquad \lambda \le x_c \quad (6)$$

and

$$K_s = \frac{D_s}{[iEI_c/(3.6\times 10^3)] + \{1/[3.6\times 10^6(\lambda - x_c)]\}\int_{x_c}^{\lambda} \gamma\sigma s(x-x_c)} \qquad \lambda > x_c \quad (7)$$

where λ = length of plot.

Equation (7) can be solved to the following simple form:

$$K_s = \frac{D_s}{[iEI_c/(3.6\times 10^3)] + [\gamma \sigma s(\lambda - x_c)/(2\times 3.6\times 10^6)]} \qquad \lambda > x_c \quad (8)$$

To find x_c, we need to determine the critical sheet flow power $(\tau V)_c$ from which x_c can be determined from Equation (9):

$$x_c = [(\tau V)_c/(\gamma \sigma_c s)](3.6\times 10^6) \quad (9)$$

where σ_c = characteristic runoff rate (mm/h) estimated by assuming that the ratio of characteristic runoff rate to characteristic rainfall intensity (σ_c/I_c) equals the ratio of characteristic runoff duration to characteristic rainfall duration $[(V_u/\sigma_c)/(V_r/I_c)]$ (Hussein & Othman 1988):

$$\sigma_c = I_c(V_u/V_r)^{1/2} \quad (10)$$

where V_u and V_r are respectively storm runoff and rainfall depths (mm).

Normally, the soil surface is covered with stones and other nonerodible materials. In this case, the flow shear stress acting on the soil surface (τ_s) will be different from the total flow shear stress (τ) (Graf 1971). To estimate τ_s, the following expression is used (Hussein 1996):

$$\tau_s = \tau(n_s/n)^{3/2} \quad (11)$$

where n_s = Manning's roughness coefficient for a bare and smooth soil surface ($m^{-1/3}$ s), and n = Manning's roughness coefficient when a surface cover is present. From Equations (9) and (11):

$$x_c = \left\{\left[(\tau_s V)_c/(n_s/n)^{3/2}\right]/(\gamma \sigma_c s)\right\}(3.6\times 10^6) \quad (12)$$

Field plot data (Rose 1988) suggest a value of 0.05 J/m^2/s for $(\tau_s V)_c$. Applying Equation (12) {[(maximum σ_c = 45.38 mm/h; Table 2)], [$n_s = 0.01$ and $n = 0.02$ (Foster *et al.* 1980); Table 1]} yields a minimum x_c value of about 19.1 m for the runoff plots data used in this study. Looking at the storm data in Table 2 reveals that only two severe-type storms during the 1989–1990 season (storms 89334 and 90073) have significant detachment by sheet flow and on the large plots only.

RESULTS AND DISCUSSION

For the same type of plots, plot to plot variability in sediment yield and runoff depth was not significant at the 95% probability level. Hence, in the subsequent discussion, average values of sediment yield and runoff depth from the replicated plots are considered.

Sediment yield from plots

Not all sediment detached on the plots is transported downslope to the collecting tank. Without a transporting agent (i.e., runoff), it was assumed that detached sediment becomes reattached to the soil surface. An expression for sediment yield is obtained by multiplying detachment rate

Table 2 | Sheet erodibility parameter (K_s) at the experimental site (S = small plots, L = large plots)

Storm Julian date	Rainfall depth (mm)	Max. 5 min intent. (mm/h)	Storm KE[a] (E) (J/m²/mm)	Init. moisture at 0–0.3 m depth (V/V)	Runoff depth (V_u) (mm)		Sediment yield (Sy) (kg/m²)		K_s^b (kg/J) × 10^{-3}	
					S	L	S	L	S	L
89334	23.5	55[c]	42.40	0.22	17	16	0.1930	0.3670	0.2618	0.4788
89344	8.5	20	10.82	0.25	2.80	2.63	0.0036	0.0037	0.0784	0.0831
90005	13	10	13.62	0.24	3.96	1.28	0.0090	0.0020	0.1059	0.0414
90023	7.5	6	16.40	0.24	2.31	0.41	0.0036	0.0004	0.0606	0.016
90046	9	9	12.89	0.26	3.45	0.39	0.0019	0.0002	0.0304	0.01
90050	10	21	17.40	0.29	5.30	3.29	0.0053	0.0032	0.0481	0.0369
90073	20	50[c]	22.70	0.29	17.00	16.00	0.0820	0.1440	0.2252	0.3570
90074	12	19	20.83	0.29	6.00	4.00	0.0250	0.0330	0.1626	0.2628
90093	10	6	16.60	0.29	1.05	0.30	0.0012	0.0007	0.0256	0.028
90096	6	24	24.00	0.30	3.67	2.98	0.0186	0.0150	0.1898	0.1699
91365	16	9	16.38	0.23	3.67	1.45	0.0031	0.0026	0.0284	0.0379
92007	11	4	12.73	0.23	2.02	0.80	0.0013	0.0013	0.0249	0.0396
92020	14.5	6	14.62	0.24	0.70	0.50	0.0006	0.0006	0.0148	0.0175
92042	7.5	6	14.67	0.30	1.38	0.54	0.0009	0.0009	0.0219	0.035
92054	10	6	13.50	0.30	1.80	0.70	0.0012	0.0011	0.0241	0.0354
92056	10	9	15.60	0.30	1.80	0.70	0.0012	0.0011	0.0208	0.0306
92057	4.2	20	14.05	0.30	1.81	0.31	0.0051	0.0006	0.1513	0.043
92066	11	10	19.82	0.30	2.73	0.28	0.0037	0.0010	0.0392	0.033

[a]Rainfall energy was estimated by breaking the storm into increments of approximately uniform intensity and calculating rainfall energy for each increment using a rainfall energy equation (Wischmeier & Smith 1958; Renard *et al*. 1997).
[b]Estimated using Equations (6), (8), and (15), $i = 0.87$ (Table 1).
[c]Severe storms.

from sheet erosion on the plot (Equation (5)) by the characteristic duration of the storm runoff event:

$$\mathrm{Sy} = D_s(V_u/\sigma_c) \times 3600 \tag{13}$$

where Sy = sediment yield from plot collected at the plot outlet expressed in kg/m^2.

Detachment by rainfall versus that by sheet flow

For the two mentioned storms during the 1989–1990 rainfall season where detachment by sheet flow was significant, sediment yield from detachment by sheet flow accounted for only 6.74 and 12.43% of total storm sediment yield for the storms of 89334 and 90073 respectively (Equations (5) and (13)). Hence, a dominant detachment by rainfall in the sheet erosion process on the plots may be assumed. This finding is supported by the fact that particle size distribution of eroded sediment in this experiment was not significantly different from that of the original soil (Hussein 1996), a case normally observed when detachment by raindrop impact is dominant (Schiettecatte *et al*. 2008).

The observed sheet erodibility parameter (K_s)

The sheet erodibility parameter for single storm events is estimated using Equations (6) and (8) where D_s is estimated from Equation (14):

$$D_s = \mathrm{Sy}/(V_u/\sigma_c)/3600 \tag{14}$$

Utilizing Equation (10), Equation (14) can be simplified to:

$$D_s = \mathrm{Sy}\left(I_c/\sqrt{V_u V_r}\right)/3600 \tag{15}$$

Table 3 | A statistical summary of the K_s and Sy values listed in Table 2

		K_s (kg/J) $\times 10^{-3}$			Sy (kg/m^2)		
	Plots	Mean	St. dev.	CV[a]	Mean	St. dev.	CV
89–90	Small	0.1188	0.0853	0.72	0.0342	0.0608	1.78
	Large	0.1484	0.1652	1.11	0.0520	0.1176	2.26
91–92	Small	0.0407	0.0452	1.11	0.0021	0.0016	0.76
	Large	0.034	0.0077	0.23	0.0012	0.0006	0.55
Both seasons	Small	0.0841	0.0793	0.94	0.0200	0.0472	2.36
	Large	0.0976	0.1338	1.37	0.0321	0.0902	2.81
Both seasons & plots		0.0908	0.1086	1.20	0.0261	0.0712	2.73

[a]Coefficient of variation (fraction).

The sheet erodibility parameter associated with detachment by raindrops' impact (and sheet flow where applicable) (K_s) for both type of plots is given in Table 2. In Table 3, a statistical summary of these K_s data is given. The dominantly high coefficients of variation for K_s values shown in Table 3 are mainly due to the high variability in the low sediment yield values used in this analysis (Table 3); such scatter in sediment yield data was observed at low runoff depth and discharge (Liu *et al.* 2005). Additional sources of variation are probably the variation in antecedent soil-water (Table 2), soil surface condition, and soil properties during the rainfall season.

As shown by Table 3, the mean K_s value for the 1989–1990 rainfall season was higher than its mean value for the 1991–1992 rainfall season for both types of plot with the difference being significant at the 95% probability level. The reason is mainly due to the absence of severe storms during the 1991–1992 rainfall season; on the same type of plots, K_s values for severe storms were generally higher compared with its values for normal storms (Table 2).

Within season differences in K_s values are also shown in Table 3. Mean K_s value was higher on the large plots compared with the small plots for the 1989–1990 rainfall season, but the opposite occurred for the 1991–1992 rainfall season; however, the difference was not significant (at the 95% probability level) in both cases (Table 3).

Table 3 also indicates that the large plots showed the highest storm to storm variation in K_s compared with the small plots for the 1989–1990 data, but the opposite occurred for the 1991–1992 data. The reason is related to the severe storms that occurred during the 1989–1990 rainfall season (Table 2); these storms increased the variability in K_s values for the large plots compared with the small plots during the 1989–1990 season (Table 2). For the 1991–1992 season data, K_s values for the large plots have considerably lower standard deviation compared with the small plots (Table 3) due probably to the diminishing runoff on the large plots (Table 2). For the two seasons combined, the difference between the means of K_s values for the large and small plots was not significant at the 95% probability level (Table 3).

K_s values in Table 2 were plotted against runoff ratio (ratio of runoff depth to rainfall depth) for the storms (Figure 2). Figure 2 shows a significant direct relationship between the two variables. Sediment yield (Sy) used to calculate K_s values is directly proportional to the sediment delivery ratio (ratio of sediment yield to gross erosion) and this delivery ratio is directly proportional to the runoff ratio (Bhunya *et al.* 2010). An exponential relationship

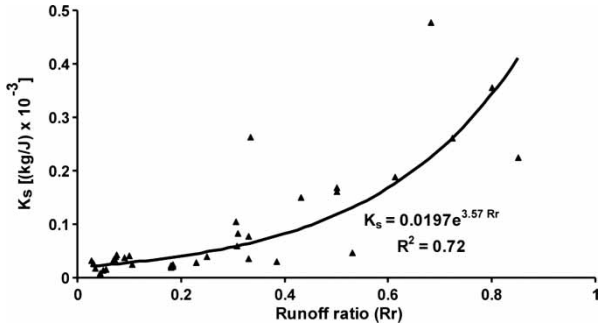

Figure 2 | Sheet erodibility vs. the ratio of runoff to rainfall for the storms in Table 2.

between the two variables (Figure 2) showed a slight improvement over a linear relationship. Two of the outliers in Figure 2 belong to the severe storms while the other two belong to normal storms characterized by a relatively high maximum 5-minute intensity (storms 90050 and 90074). High intensity storms result in a sediment-laden sheet flow which involves interaction between detachment and transport mechanisms of soil particles not considered in this analysis (Hussein 1996).

K_s values fluctuate during the rainfall season without apparent trend. After the initial tillage, surface crust developed on the plots during the rainfall season (Hussein *et al.* 2010). Soil surface sealing and crusting tend to reduce soil susceptibility to detachment due to soil consolidation caused by raindrop impact which caused an increase in the soil shear strength (Onstad *et al.* 1984; Bradford *et al.* 1987; Alberts *et al.* 1995). Such effect was not evident in this study, due probably to the increase in surface runoff resulting from the decrease in soil basic infiltration rate caused by soil surface sealing and crusting.

The representative sheet erodibility parameter

A representative sheet erodibility parameter for a given soil may be needed for use in sheet erosion modeling. Table 2 indicates a discrepancy in K_s values between severe and normal rainfall events for both types of plots. Severe storms usually produce a short duration sediment-laden flow as mentioned earlier while soil loss from normal storms occurs mainly during the period of maximum rainfall intensity (Hussein 1996). The coefficient of skewness for the K_s values in Table 2 was 2.04; this high coefficient of skewness is caused by a few high K_s values, mainly from severe storms. Accordingly, the two-parameter lognormal probability distribution gave a reasonable fit to the K_s values in Table 2 (Figure 3). For such skewed probability distribution, the geometric mean and the median may prove useful for a representative sheet erodibility parameter. The geometric mean and the median for the K_s data in Table 2 are 0.0533×10^{-3} and 0.0582×10^{-3} kg/J, respectively; their average of 0.056×10^{-3} kg/J is taken as the representative K_s value at the experimental site. Figure 3 shows that K_s value is less than 0.1×10^{-3} kg/J in about 70% of the cases.

Another approach used for calculating a representative sheet erodibility parameter is by optimization. In this case, the observed sediment yield (Sy) was converted from a storm basis to an instantaneous rate basis. To obtain a representative K_s value, the sum of these instantaneous sediment yield values was divided by the sum of the effective sheet flow power integrated along the slope (Equation (8)):

$$\overline{K}_s = \frac{\sum_{j=1}^{m} \left(\mathrm{Sy}\, I_c/\sqrt{V_u V_r}\right)_j}{\sum_{j=1}^{m} \{(iEI_c) + [\gamma\sigma s(\lambda - x_c)/(2\times10^3)]\}_j} \quad (16)$$

where $\overline{K}_s =$ the representative sheet erodibility parameter (kg/J) and $m =$ number of storms involved in the computation. However, including both severe and normal-type storms in the calculation of $\overline{K}_s$ by Equation (16) will bias the fitting of relationships. For normal storms, estimated

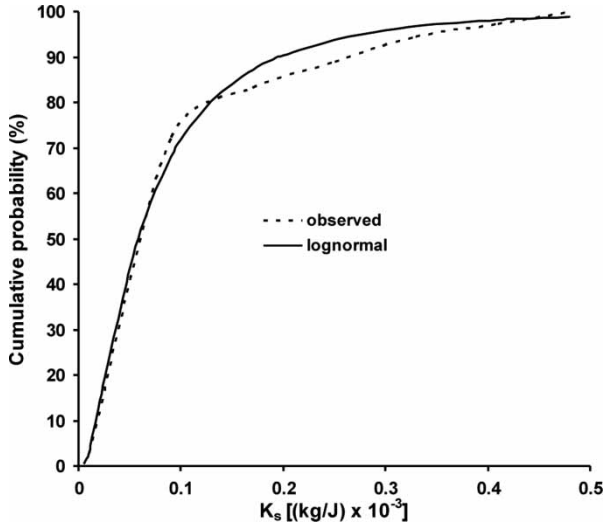

Figure 3 | Cumulative probability of sheet erodibility values listed in Table 2.

$\overline{K}_s$ value was 0.1×10^{-3} kg/J for both types of plots. For severe storms, estimated $\overline{K}_s$ values were 0.25×10^{-3} and 0.44×10^{-3} kg/J for the small and the large plots, respectively. Hence, this approach may not be suitable for calculating a representative K_s value when the K_s values from individual storms are substantially skewed.

SUMMARY AND CONCLUSIONS

Basic sheet erosion concepts were used to evaluate a sheet erodibility parameter needed for the application of water erosion models in a region of dominantly low intensity rain. Data from fallowed natural runoff plots in northern Iraq showed a dominant detachment by rainfall in the upper portion of gentle slopes due to the low sheet flow rate. Calculated sheet erodibility parameter showed a substantial storm by storm variability and direct relationship with the ratio of runoff to rainfall. The parameter nearly follows a lognormal probability distribution; this probability distribution was then used to obtain a representative sheet erodibility value of 0.056×10^{-3} kg/J for use at the experimental site.

ACKNOWLEDGEMENTS

Thanks go to M. M. Awad and A. S. Abdul-Jabbar for participating in data collection used in this study.

REFERENCES

Alberts, E. E., Nearing, M. A., Weltz, M. A., Risse, L. M., Pierson, F. B., Zhang, X. C., Laflen, J. M. & Simanton, J. R. 1995 Soil component. In: *USDA - Water Erosion Prediction Project Documentation* (D. C. Flanagan & M. A. Nearing, eds). USDA-ARS National Soil Erosion Research Laboratory, West Lafayette, IN, USA, pp. 7.1–7.47.

Beasley, D. B., Monke, E. J. & Huggins, L. F. 1980 ANSWERS: a model for watershed planning. *Trans. Am. Soc. Agric. Eng.* **23**, 839–944.

Bhunya, P. K., Jain, S. K., Sing, P. K. & Mishra, S. K. 2010 A simple conceptual model of sediment yield. *Water Resour. Manage.* **24**, 1697–1716.

Bradford, J. M., Ferris, J. E. & Remley, P. A. 1987 Interrill soil erosion processes: I. Effect of surface sealing on infiltration, runoff, and soil splash detachment. *Soil Sci. Soc. Am. J.* **51**, 1566–1571.

Brodie, I. M. & Egodawatta, P. 2011 Relationships between rainfall intensity, duration and suspended particle washoff from an urban road surface. *Hydrol. Res.* **42**, 239–249.

Edwards, K. 1985 Preliminary analysis of runoff and soil loss from selected long term plots in Australia. In: *Soil Erosion and Conservation* (S. A. El-Swaify, W. C. Moldenhauer & A. Lo, eds). Soil and Water Conservation Society, Ankeny, IA, USA, pp. 472–479.

Foster, G. R. 1982 Modeling the erosion process. In: *Hydrologic Modeling of Small Watersheds* (C. T. Haan, H. P. Johnson & D. L. Brakensiek, eds). Am. Soc. Agric. Eng., St. Joseph, MI, USA, pp. 297–370.

Foster, G. R., Huggins, L. F. & Meyer, L. D. 1968 Simulation of overland flow on short field plots. *Water Resour. Res.* **4**, 1179–1187.

Foster, G. R., Lane, L. J. & Nowlin, J. D. 1980 A model to estimate sediment yield from field-sized areas: Selection of parameters values. In: *CREAMS – a field scale model for Chemicals, Runoff and Erosion from Agricultural Management Systems,* vol. II, User Manual (W. G. Knisel, ed.). USDA-ARS-Conservation Research Report No. 26, Washington, DC, USA, pp. 193–281.

Foster, G. R., Lane, L. J., Nowlin, J. D., Laflen, J. M. & Young, R. A. 1981 Estimating erosion and sediment yield on field sized areas. *Trans. Am. Soc. Agric. Eng.* **24**, 1253–1262.

Graf, W. H. 1971 *Hydraulics of Sediment Transport*. McGraw-Hill, New York, NY, USA.

Gumiere, S. J., Bissonnais, Y. L. & Raclot, D. 2009 Soil resistance to interrill erosion: model parameterization and sensitivity. *Catena* **77**, 274–284.

Hussein, M. H. 1996 An analysis of rainfall, runoff and erosion in the low rainfall zone of northern Iraq. *J. Hydrol.* **181**, 105–126.

Hussein, M. H. 1998 Water erosion assessment and control in northern Iraq. *Soil Tillage Res.* **45**, 161–173.

Hussein, M. H. & Othman, A. K. 1988 Soil and water losses in a low intensity rainfall region in Iraq. *Hydrol. Sci. J.* **33**, 257–267.

Hussein, M. H., Awad, M. M. & Abdul-Jabbar, A. S. 1994 Predicting rainfall-runoff erosivity for single storms in northern Iraq. *Hydrol. Sci. J.* **39**, 535–547.

Hussein, M. H., Awad, M. M. & Abdul-Jabbar, A. S. 2010 Effect of surface crust on rainfall infiltration in an Aridisol in northern Iraq. *European Water* **32**, 25–34.

Jarjees, E. A., El-Swaify, S. A., Chan-Halbrendt, C., Fares, A. & Zaghloul, S. 2006 Conservation and environmental issues in revitalizing Iraqi Agriculture. In: *Proc. 14th Conference of the International Soil Conservation Organization* (M. Saber, ed.). ISCO, Marrakesh, Morocco (May 14–19), p. 207.

Kinnell, P. I. A. 1993 Runoff as a factor influencing experimentally determined interrill erodibilities. *Aust. J. Soil Res.* **31**, 333–342.

Laflen, J. M., Elliot, W. J., Simanton, J. R., Holzhey, C. S. & Kohl, K. D. 1991 WEPP soil erodibility experiments for rangeland and cropland soils. *J. Soil Water Conserv.* **46**, 39–44.

Liu, Q. Q., Singh, V. P. & Xiang, H. 2005 Plot erosion model using Gray Relational Analysis method. *J. Hydrol. Eng. ASCE* **10**, 288–294.

Moore, I. D. & Burch, G. J. 1986 Physical basis of the length-slope factor in the Universal Soil Loss Equation. *Soil Sci. Soc. Am. J.* **50**, 1294–1298.

Morgan, R. P. C., Quinton, J. N., Smith, R. E., Govers, G., Poesen, J. W. A., Auerswald, K., Chisci, G., Torri, D. & Styczen, M. E. 1998 The European Soil Erosion Model (EUROSEM): a dynamic approach for predicting sediment transport from fields and small catchments. *Earth Surf. Proc. Land.* **23**, 527–544.

Nearing, M. A., Foster, G. R., Lane, L. J. & Finkner, S. C. 1989 A process-based soil erosion model for USDA – Water Erosion Prediction Project technology. *Trans. Am. Soc. Agric. Eng.* **32**, 1587–1593.

Onstad, C. A., Wolf, M. L., Larson, C. L. & Slack, D. C. 1984 Tilled soil subsidence during repeated wetting. *Trans. Am. Soc. Agric. Eng.* **27**, 733–736.

Partheniades, E. 1972 Results of recent investigations on erosion and deposition of cohesive sediments. In: *Sedimentation (Einstein)* (H. W. Shen, ed.). Water Resources Publications, Fort Collins, CO, USA, Ch. 20.

Pettersen, S. 1958 *Introduction to Meteorology*. 2nd edn, McGraw-Hill, New York, NY, USA.

Reichert, J. M., Norton, L. D., Favaretto, N., Huang, C. & Blume, C. E. 2009 Settling velocity, aggregate stability, and interrill erodibility of soils varying in clay mineralogy. *Soil Sci. Soc. Am. J.* **73**, 1369–1377.

Renard, K. G., McCool, D. K., Cooley, K. R., Foster, G. R., Istok, J. D. & Mutchler, C. K. 1997 Rainfall-runoff erosivity factor (R). In: *Predicting Soil Erosion by Water: A Guide to Conservation Planning With the Revised Soil Loss Equation (RUSLE)* (K. G. Renard, G. R. Foster, G. A. Weesies, D. K. McCool & D. C. Yoder, compilers). Agric. HB No. 703. USDA, Washington, DC, USA, pp. 19–64.

Romero, C. C., Stroosnijder, L. & Baigorria, G. A. 2007 Interrill and rill erodibility in the northern Andean Highlands. *Catena* **70**, 105–113.

Rose, C. W. 1988 Research progress on soil erosion processes and a basis for soil conservation practices. In: *Soil Erosion Research Methods* (L. Lal, ed.). Soil and Water Conservation Society, Ankeny, IA, USA, pp. 119–139.

Rovey, E. W. & Woolhiser, D. A. 1977 *A Distributed Kinematic Model of Upland Watersheds*. Hyd. Paper No. 23. Colorado State University, Fort Collins, CO, USA.

Schiettecatte, W., Gabriels, D., Cornelis, W. M. & Hofman, G. 2008 Enrichment of organic carbon in sediment transport by interrill and rill erosion processes. *Soil Sci. Soc. Am. J.* **72**, 50–55.

Toorman, E. A. 2001 Cohesive sediment transport modelling: European perspective. In: *Coastal and Estuarine Sediment Processes* (H. McAnally & A. J. Mehta, eds). Elsevier Science, New York, NY, USA, pp. 1–16.

Truman, C. C. & Bradford, J. M. 1995 Laboratory determination of interrill soil erodibility. *Soil Sci. Soc. Am. J.* **59**, 519–526.

Utley, B. C. & Wynn, T. M. 2008 Cohesive soil erosion: theory and practice. In: *Proceedings of the ASCE World Environmental and Water Resources Congress (Ahupua'a)* (R. W. Babcock Jr & R. Walton, eds). Honolulu, Hawaii, May 12–16, pp. 1–10.

Wei, H., Nearing, M. A., Stone, J. J., Guertin, D. P., Spaeth, K. E., Pierson, F. B., Nichols, M. H. & Moffet, C. A. 2009 A new splash and sheet erosion equation for rangelands. *Soil Sci. Soc. Am. J.* **73**, 1386–1392.

Wischmeier, W. H. & Smith, D. D. 1958 Rainfall energy and its relationship to soil loss. *Trans. Am. Geophys. Union* **39**, 285–291.

Yang, C. T. 1972 Unit stream power and sediment transport. *J. Hyd. Div. Am. Soc. Civil Eng.* **98**, 1805–1826.

Yang, C. T. 1973 Incipient motion and sediment transport. *J. Hyd. Div. Am. Soc. Civil Eng.* **99**, 1679–1704.

Zhang, G. H., Liu, B. Y., Liu, G. B., He, X. W. & Nearing, M. A. 2003 Detachment of undisturbed soil by shallow flow. *Soil Sci. Soc. Am. J.* **67**, 713–719.

Zhang, X. C., Nearing, M. A., Miller, W. P., Norton, L. D. & West, L. T. 1998 Modeling interrill sediment delivery. *Soil Sci. Soc. Am. J.* **62**, 438–444.

First received 28 January 2012; accepted in revised form 2 November 2012. Available online 16 January 2013